Late Cretaceous to recent ocean-bottom currents in the SW Pacific Gateway, southeastern Chatham Rise, New Zealand

Lara Steinbrink[a,*], Karsten Gohl[a], Florian Riefstahl[a], Bryan Davy[b], Lionel Carter[c]

[a] *Alfred Wegener Institute Helmholtz-Centre for Polar and Marine Research, Bremerhaven, Germany*
[b] *GNS Science, Lower Hutt, New Zealand*
[c] *Victoria University Wellington, Wellington, New Zealand*

ARTICLE INFO

ABSTRACT

Sedimentary drifts archive the history of the ocean-bottom current dynamics. Bottom currents associated with the Pacific Deep Western Boundary Current (DWBC) along the submarine continental margin off southern and eastern New Zealand are of particular interest because of their potential to contain records of changes in the SW Pacific circulation. Analysis of multi-channel seismic reflection data from the RV Sonne expedition SO246 together with earlier seismic data enabled us to reconstruct bottom currents and map sediment deposits along the southeastern Chatham Rise margin for the past 80 million years. The seismic records are supplemented by sub-bottom profiler and bathymetric data, which provide detailed information on the youngest stratigraphy, sedimentary structures and bathymetry. This approach allows time-dependent mapping of sedimentary deposits and reconstruction of current regimes. The opening of the Tasmanian Gateway in the early Oligocene led to the development of the DWBC, which influenced regional sedimentary processes. However, the occurrence of bottom current activity prior to opening the Tasmanian Gateway suggests the existence of a proto-DWBC. Increased bottom current activity in the Miocene indicates a change to a more dynamic circulation regime in the SW Pacific, consistent with intensification of Antarctic glaciation and increased Antarctic Bottom Water formation. Plio/Pleistocene records indicate a weakening of the bottom-water energy along the Chatham Rise margin. Overall, sediment deposition was widespread before gateway opening, almost non-existent in the Oligocene and sparse in the Neogene.

1. Introduction

The heat transport by the global ocean circulation influences much of the Earth's climate. The Southern Ocean circulation with its cold, deep Antarctic Bottom Water (AABW) and lower Circumpolar Deep Water (LCDW) are key parts of this system (Orsi et al., 1999). These waters are fed into the world ocean by Deep Western Boundary Currents (DWBC), the largest of which flows north-eastward along the southeastern continental margins of the Campbell Plateau and Chatham Rise of New Zealand and onto the central Pacific Ocean (Fig. 1) (McCave and Carter, 1997; Carter et al., 1996). Today, a suite of sediment drifts and contourites, deposited along the lower slope and continental rise of the Campbell Plateau and Chatham Rise, represents records of the development of ocean-bottom currents since the early Oligocene (Carter et al., 2004). Large-scale ocean circulation processes such as changes in the deep-water formation and the opening of ocean gateways are archived in these sediment accumulations.

In this study, we reconstruct ocean-bottom currents along the southeastern margin of the Chatham Rise for the past 80 million years by seismic investigations of sedimentary successions influenced by paleo-oceanographic processes. A main component is the mapping and interpretation of sedimentary sequences in relation to previous research results as well as a time-dependent reconstruction of past ocean currents. Furthermore, the verification of the so-called 'Eastern New Zealand Oceanic Sedimentary System' (ENZOSS) model developed by Carter et al. (1996), as well as the refinement and extension of this scenario are discussed. The key of this work is based on the data of several standard multi-channel seismic reflection profiles, which were collected along the southeastern Chatham Rise margin as part of the science program during RV Sonne expedition SO246 in early 2016 (Fig. 2). Furthermore, sub-bottom profiler and bathymetric data provide complementary information.
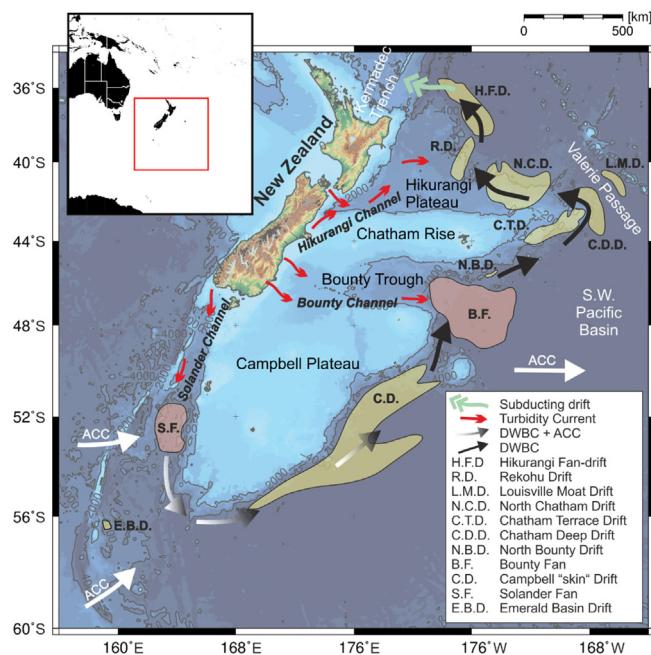
Fig. 1. Overview of southeastern New Zealand region with its Campbell Plateau and Chatham Rise. Major sediment drifts and ocean current paths in the Neogene are marked. The map illustrates the ENZOSS model of Carter et al. (2004). ACC = Antarctic Circumpolar Current, DWBC = Deep Western Boundary Current.
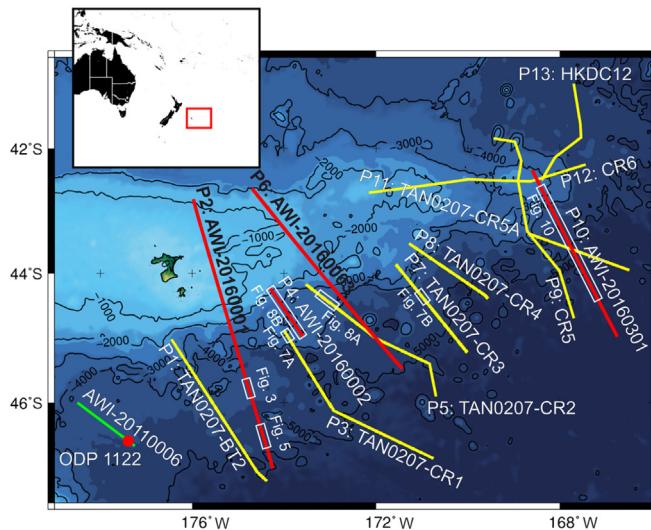
Fig. 2. Eastern Chatham Rise and its margins with locations of seismic lines and ODP Site 1122. Red lines mark the seismic reflection lines acquired during RV Sonne cruise SO246; yellow lines mark pre-existing seismic reflection lines of the New Zealand UNCLOS project; green line marks a seismic reflection line acquired during RV Sonne cruise SO213; white boxes mark profile sections presented in this paper. (For interpretation of the references to color in this figure legend, the reader is referred to the web version of this article.)

2. Regional setting

The present shape of the Chatham Rise largely formed during the break-up of East Gondwana, which led to the separation of Australia and Zealandia (New Zealand and its submarine continental crust) from Antarctica in the Cretaceous between 90 and 80 Ma (e.g. Whittaker et al., 2007; Eagles et al., 2004) or even earlier (e.g. Whittaker et al., 2013; Mortimer et al., 2019). Chatham Rise was the first block of Zealandia to separate from the West Antarctic margin at 90–83 Ma

(Larter et al., 2002; Eagles et al., 2004; Wobbe et al., 2012). After the opening of the Tasmanian Gateway, which developed due to the separation of Tasmania and South Tasman Rise from East Antarctica, medium-deep and deep water have been able to pass through since the early Oligocene (e.g. Kennett et al., 1972; Stickley et al., 2004). As a result, the Antarctic Circumpolar Current (ACC) developed, and so did supposedly the Pacific Deep Western Boundary Current. The DWBC is the main deep-water inflow (> 2000 m depth) into the Pacific Ocean via the Pacific Gateway off the continental margin east of New Zealand (Carter et al., 1996; Horn and Uenzelmann-Neben, 2015). South-east of the Campbell Plateau, it is over-ridden and dominated by the ACC, which uncouples at the mouth of Bounty Trough (Fig. 1) (Carter and Wilkin, 1999). The DWBC continues its way rounding the eastern flank of the Chatham Rise and diverting northwards along the eastern edge of the Hikurangi Plateau and Tonga-Kermadec Trench (Whitworth et al., 1999). Horn and Uenzelmann-Neben (2015) suggested the possibility of a proto-DWBC that existed even before the Tasmanian Gateway opening.

After the inception of the ACC and the DWBC, deposition of deep-sea sedimentary drifts along the Campbell Plateau and Chatham Rise margins intensified (Carter et al., 2004). This was the beginning of the development of the ENZOSS, a model to describe the interrelationship between provenance, transport and deposition of sediments in this region (Fig. 1) (Carter et al., 1996). They suggested that sediments from the mountainous regions of the New Zealand convergent plate boundary were transported by turbidity currents through deep-sea channel and fan systems into the path of the DWBC. These sediments are then carried northwards within this current system and deposited as a series of sediment drifts, whose sediments can be reworked and some of it finally consumed by subduction at the same plate boundary, in which it originates, after transport of over 3500 km (Carter et al., 1996).

Large volumes of reworked sediments are now incorporated in deep-sea contourite drifts formed by deposition from DWBC and represent the impact of the Tasmanian Gateway opening, changes in the thermohaline system of the Pacific Ocean, development of Antarctic ice sheets and the tectonic evolution of the New Zealand plate boundary (Carter and McCave, 1994; Carter et al., 2004). Additionally, these events are overprinted with effects of orbital forcing on sediment supply, abyssal sedimentation and current flow, which increase the complexity of the ENZOSS (Carter et al., 2004). The investigation of sediment drifts in the Chatham Rise section of the Pacific Gateway provides a more detailed understanding of these processes and their impacts since the break-up of eastern Gondwana.

3. Data acquisition

Our database consists of four new seismic reflection profiles (Fig. 2; P2, P4, P6 and P10), collected during the RV Sonne expedition SO246 in early 2016 (Gohl and Werner, 2016). These profiles are located along the southeastern margin of the Chatham Rise in 300–5300 m water-depth and show sediment deposits of various size, shape and internal structure. An additional nine pre-existing seismic reflection profiles, which were acquired in the framework of the New Zealand UNCLOS (United Nations Convention on the Law of the Sea) project (Fig. 2), as well as sub-bottom profiler and swath-bathymetry data from SO246, were also used.

The seismic reflection data of SO246 were acquired with a 3000-m long digital streamer of 240 channels. Profiles P2 and P6 were shot with an array of 6 G-Guns (51 l/3120 in^3) using a shot interval of 20 s. Profile P10 was shot with an array of 8 G-Guns with a shot interval of 60 s (for simultaneous seismic refraction/wide-angle reflection recordings with ocean-bottom seismometers, which is subject to a different study; Riefstahl et al., 2020), and P4 was shot with an array of 4 G-Guns with a shot interval of 20 s. Standard data processing was performed with Paradigm Echos™ software and included spherical

divergence correction, velocity analysis, normal move-out correction, stacking, finite difference time-migration, bandpass filtering of 5/15–150/200 Hz, and muting of the water column.

We also used data from (i) the parametric sediment-echosounding system Teledyne Atlas Parasound DS-III-P70 for the uppermost sediments and (ii) multibeam bathymetric data collected via a Kongsberg Simrad EM122 system.

4. Seismic observations and interpretation

The processed seismic reflection profiles P2, P4, P6 and P10 provide high-quality insight into subsurface structure and stratigraphy. Various units were defined in each profile and combined with units interpreted on the New Zealand UNCLOS project profiles to create a quasi-3D understanding of the study area. Due to the lack of sufficient crossing profiles, we based our seismic correlation and interpretation between profiles on tying seismic characteristics. Four main seismic units and their bounding main reflectors were identified and marked between acoustic basement and seafloor. The identification of the acoustic basement was aided by P-wave velocity models from seismic refraction data (Riefstahl et al., 2020). As deep drill-core data do not exist directly in the study area, it is not always possible to distinguish the crystalline basement from old meta-sediments that may overlie the basement and have similar acoustic impedance. Using a representative section of seismic profile P2 (Fig. 3, Table 1), we described selected horizons along the profiles. Additionally, Parasound records were utilized as supplementary, high-resolution information on the uppermost sequences. The Parasound data show up to three subdivisions of the topmost unit in specific parts of the profiles (Fig. 4, Table 2). Main reflectors were named Southeastern Chatham Rise SCR 1 to SCR 6 upwards from the basement. We named the main Units A to D from the seafloor downwards and Sub-units A1 to A3 and D1 to D2, respectively, from the bottom of the units upwards.

Four main units were identified in the sedimentary sequence, which is shown in a type section of profile P2 (Fig. 3). The units rest on acoustic basement that is marked by a discontinuous, high amplitude reflector at maximum depth of 1300 ms two-way travel time (TWT) below the seafloor. Seamounts disrupt the sedimentary section in places.

Unit D is the lowermost unit and overlies the assumed basement. It
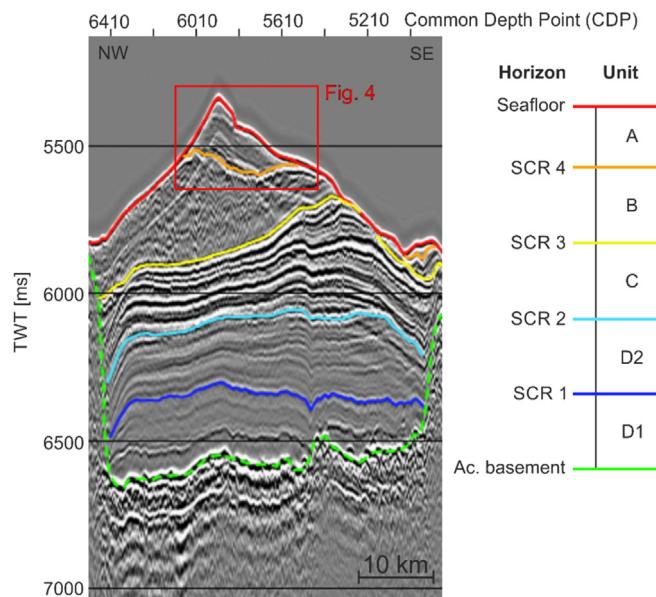
Fig. 3. Stratigraphic reference of seismic units in a chosen type section of profile P2. Seismic attributes can be found in Table 1.

can be subdivided into sub-units, D1 with a maximum thickness of 290 ms TWT and D2 with a maximum thickness of 310 ms TWT. Both are characterized by subparallel, discontinuous reflectors and in some cases acoustic transparency. They are separated by a comparatively strong reflection (SCR 1).

Unit C overlies Unit D, showing onlap and downlap structures on basal reflector SCR 2. An erosional truncation can be found where Unit C outcrops. It is characterized by high amplitude reflectors, that become less intense down-section. In Fig. 3 reflectors are parallel bedded, whereas in other cases, they are less continuous. Unit thickness reaches up to 430 ms TWT.

Unit B is bounded by a strong basal reflector SCR 3, and is distinguished by chaotic, discontinuous, wavy bedded reflectors with low amplitude. The thickness varies considerably up to 390 ms TWT. Erosional truncations can be found where Unit B outcrops, and an unconformity (SCR 4) marks the boundary with Unit A.

Unit A overlies Unit B with onlap and downlap configurations. Internal reflectors are better resolved by Parasound and show closely spaced, continuous and subparallel reflectors, which are wavy bedded. Unit A can be subdivided into three sub-units, each separated by reflectors SCR 5 and SCR 6 and often shows internal onlaps. Unit A reaches a thickness of 230 ms.

The result of a time-to-depth conversion shows a depth range of the section of profile P2 between 4030 m and 4230 m. In comparison with the same profile illustrated in TWT the Units A and B look quite similar and reach maximum thicknesses of 170 m (Unit A) and 330 m (Unit B). The underlying Units C and D have maximum thicknesses of 420 m and 630 m respectively.

A stratigraphic classification of the sedimentary units is essential for a time-dependent reconstruction of ocean currents and sediment deposition. Since no drill core data exist directly from the work area, we correlated our seismic units using comparable seismic reflection pattern characteristics, with the seismic stratigraphy developed by Carter et al. (1994) and Horn and Uenzelmann-Neben (2015), which is based on seismic profile AWI-20110006 crossing ODP Leg 181 Site 1122 located on the Bounty Fan (Figs. 1; 2) and oil exploration wells. Table 3 shows the resultant stratigraphic age model for the identified sedimentary units. Units A to D are assumed to represent the Units A to D determined in Horn and Uenzelmann-Neben (2015). Units A and B were drilled at ODP Site 1122 and described by Carter et al. (1999). Unit A compares with Unit I from Carter et al. (1999), dated from the early Pleistocene to recent times and consists of terrigenous sediments, which have been transported by turbidity currents via the Bounty Channel (Horn and Uenzelmann-Neben, 2015). At Site 1122 this unit shows subparallel, strong reflections onlapping the underlying unit. After Horn and Uenzelmann-Neben (2015) the Unit B can be linked to Unit II and Unit III from Site 1122, which are dated from the middle Miocene to middle Pleistocene. Unit II comprises bioturbated, pelagic and hemipelagic sediments, interbedded with current-laminated deposits (Carter et al., 1999). A hiatus at 10.4 to 5 Ma defines the boundary to Unit III, which shows the same lithology but a coarser grain size (Horn and Uenzelmann-Neben, 2015). Horn and Uenzelmann-Neben (2015) describe Unit B between middle and outer Bounty Trough as chaotic, with subparallel medium amplitude reflections in the outer Bounty Trough. A hiatus from Eocene to middle Miocene age, called the 'Marshall Paraconformity' (Carter et al., 2004) separates Unit B from Unit C, and is apparent in the seismic reflection data as a strong amplitude erosional unconformity. Units C and D, which were not drilled at Site 1122 are dated by correlation to oil exploration wells from the Canterbury Basin and the Great South Basin (Carter et al., 1994; Horn and Uenzelmann-Neben, 2015). There, Unit C comprises hemipelagites and calcareous biopelagites (Carter et al., 1994). Horn and Uenzelmann-Neben (2015) date this unit, which is characterized by medium amplitude, equally spaced reflectors, from Paleocene to Eocene age. Carter et al. (1994) describe Unit D as non-marine breccia-conglomerates with thick immature coal measure sequences. This unit is characterized by

Table 1

Seismic attributes of the units in a chosen section of profile P2 (Fig. 3).

Unit	Attributes	Thickness
A	Parallel, strong and continuous reflectors; wavy bedded; closely spaced; onlap (CDP 4900)/downlap (CDP 5600–5800) on B; erosional truncations on both sides	< 170 m
B	Irregular, discontinuous, wavy/chaotic reflectors; acoustically transparent; toplap and erosional truncation at CDP 5300–5600	< 330 m
C	Strong, rare and parallel reflectors; sometimes internal onlaps/downlaps and erosional truncations (CDP 5100–5300)	< 420 m
D2	Subparallel, semicontinuous reflectors; downwards tending to acoustical transparency	< 310 m
D1	Subparallel, semicontinuous, rare and faint reflectors; tending to acoustical transparency	< 320 m
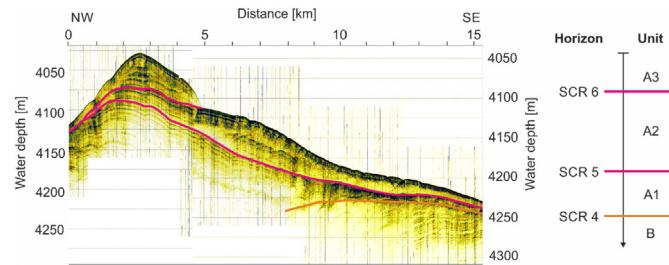
Fig. 4. Stratigraphic reference of Parasound units in a chosen section of profile P2. Seismic attributes can be found in Table 2.

Table 2

Seismic attributes of the sub-units in the Parasound data from the chosen section of profile P2 (Fig. 4).

Unit	Attributes	Thickness
A3	Subparallel reflectors; downlap on A2	< 45 m
A2	Subparallel, partly strong reflectors; downwards tending to acoustical transparency; partly wavy bedded	< 50 m
A1	Subparallel, partly strong reflectors; wavy bedded	< 95 m

Table 3

Stratigraphic age model of sedimentary units in the work area, based on seismic stratigraphy by Horn and Uenzelmann-Neben (2015).

Unit	Age (Ma)	Seismic characteristics
A	Recent - 1.7	Subparallel closely spaced reflectors, onlapping underlying unit
B	1.7–19.5	Chaotic reflectors
C	33.7–56	High amplitude equally spaced reflectors
D2	56–65	Medium amplitude reflectors to acoustically transparent zones
D1	65–80	

medium amplitude reflectors in the upper part to almost reflection-free sections in the lower part and is dated from Cretaceous to Paleocene age (Horn and Uenzelmann-Neben, 2015). The upper part is interpreted to represent Unit D2, while the lower part is comparable to Unit D1 of our work. The boundary between both sub-units is probably represented by reflector R5 of Horn and Uenzelmann-Neben (2015), which they describe as a reflector of continuous varying amplitude, dated to 65 Ma.

5. Sediment drift formation and paleo-circulation

5.1. Oceanographic and sedimentary conditions from 80 to 33.7 Ma

Carter et al. (1994) describe deposits formed before the opening of the Tasmanian Gateway, as post-rift or rift-fill sediments. Sedimentary units found in the study area on top of the presumed Early Cretaceous or older metasedimentary basement, occur as a typical sedimentary drape, which suggests a post-rift accumulation.

Both Units C and D show subparallel reflectors, which often follow the basement structure (Fig. 5). This indicates sediment deposition which is draped onto the post-breakup faulted and intruded oceanic

basement. Furthermore, as the layers are mainly regularly bedded, pelagic/hemipelagic deposition likely prevailed without erosive currents. However, in several areas internal discontinuities onlap, downlap and erosional truncations (see Fig. 5, Common Depth Point (CDP) 1400 to 2400) indicate bottom current activity before the opening of the Tasmanian Gateway at 33.5 Ma (Exon et al., 2004; Carter et al., 2004). Horn and Uenzelmann-Neben (2015) suggest the existence of a proto-DWBC passing the work area in north-eastern direction and driven by cold deep-water flows in the early Paleocene, which could explain erosional and current-controlled features noted in this study (Fig. 5). This is consistent with a numerical simulation by Sijp et al. (2011), which describes a southern hemisphere subpolar circulation with a clockwise rotation in the SW Pacific Ocean prior to the opening of the Tasmanian Gateway. Bottom disturbing currents associated with meso-scale eddies might have created areas of local erosion as found in several profiles. Our observations indicate that sediment deposition, especially in the south-western part of the study area, was influenced by a presumed proto-DWBC (Fig. 6), indicating a strong circulation of the southern Pacific Ocean despite its partial isolation.

5.2. Oceanographic and sedimentary conditions from 33.7 to 19.5 Ma

The opening of the Tasmanian Gateway, dated to 33.5 Ma, led to the initiation of the ACC and following this, widespread erosion and the formation of the 'Marshall Paraconformity' (Kennett et al., 1972; Carter and Landis, 1972; Exon et al., 2004; Carter et al., 2004). Evidence for this event occurs in all our profiles. Downslope areas of several profiles show a strong erosional influence of bottom currents with comparative high velocities, as shown in Fig. 7A. The downslope area of profile P3, which is located in the south-western part of the study area, shows an erosional surface of Unit C as well as a moat around the seamount (Fig. 7A). Erosional truncations next to seamounts and ridges probably reflect topographic intensification of the ancestral DWBC. In profile P7 Unit C is highly eroded and is sometimes removed to allow erosion extend into Unit D (Fig. 7B). This effect was probably caused by rapid bottom currents, which intensified against the western boundary presented by Chatham Rise slope at around 44°S to 44.2°S and 171°W to 172°W (see Fig. 6). Unit C shows very small thicknesses of sometimes < 100 m in the easternmost profiles P9 to P13 (e.g. Fig. 10), which leads to the conclusion that after the opening of the Tasmanian Gateway current velocities were high across the flow path. This was probably affected by a steep slope in the area of P9, P10, and P11 (Fig. 6) as well as the narrowing of the DWBC through Valerie Passage (Fig. 1) (Carter and McCave, 2002). In summary, there has been little or no deposition of drift deposits in the region from 33.7 to 19.5 Ma (early Oligocene to mid Miocene) due to erosive bottom currents.

5.3. Oceanographic and sedimentary conditions from 19.5 to 1.7 Ma

An unconformity of widespread erosion (SCR3) marks the basal boundary to Unit B, whose deposition age ranges from 1.7 to 19.5 Ma (Horn and Uenzelmann-Neben, 2015). This unit is distinguished from the underlying units by a different distribution and seismic characteristics. Chaotic, wavy internal reflectors (Fig. 8A) indicate often varying current conditions. Uenzelmann-Neben et al. (2009) suggest a major
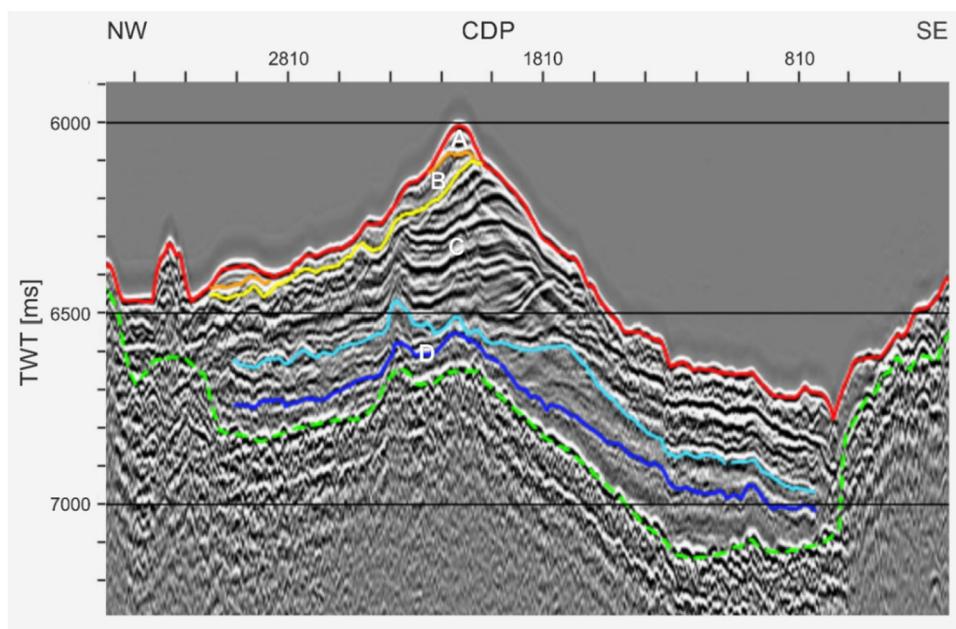
Fig. 5. A section of profile P2 with seismic interpretation. Units C and D show subparallel reflectors, which often follow the basement structure. However, internal onlaps at the boundary from Unit D1 to D2 (CDP 1800 to 1900) and in Unit C (CDP 1800 to 1850) as well as an erosional surface of Unit D from CDP 1400 to 2400 point to the occurrence of regional bottom current activity prior to the opening of the Tasmanian Gateway.
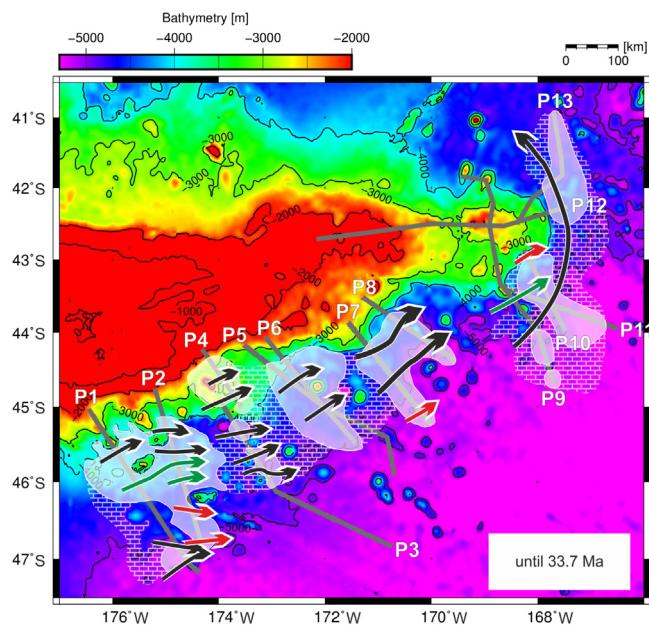
Fig. 6. Interpolated locations of sediment deposits of Unit C and D until the opening of the Tasmanian Gateway are illustrated by white areas. Brick-pattern areas represent interpolations between those areas. Ocean current locations after the opening of the Tasmanian Gateway are illustrated by black arrows. Locations of a proto-DWBC are shown by red arrows, and current locations both before (proto-DWBC) and after the opening of the Tasmanian Gateway are illustrated by green arrows. Profile lines are shown in grey. (For interpretation of the references to color in this figure legend, the reader is referred to the web version of this article.)

modification of Bounty Trough sedimentation and refer to internal onlaps, which indicate changes in the sedimentary environment and periods of erosion or non-deposition. Internal onlaps also occur in Unit B (Fig. 8A), suggesting similar oceanographic conditions off Chatham Rise, namely, frequent reworking and redeposition under a strong but variable DWBC. This is supported by ODP Site 1122, which has Miocene ripple drift and laminated sands, locally enriched with detrital chlorite that appears to come from sediments cored at the foot of Campbell Plateau Site 1121 (Carter et al., 2004).

Distinctly varying thicknesses of Unit B and small areas of non-deposition or erosion and moating next to seamounts in the area between P1 and P4 probably reflect localised topographic intensification of the flow (Fig. 8B). Possible current paths and current channels, which have affected the deposition of Unit B, are illustrated in Fig. 9 (channels a–e). Sedimentary structures in these profiles compared with each other and the bathymetric data allow an interpolation of depositional areas between the profiles P1 and P2 and the surrounding area (Fig. 9).

Between the profiles P3 and P6 deposition of Unit B only occurs at the slope and is characterized by chaotic internal reflectors and a very erosive surface at the top of the unit (Fig. 8A). It is possible that submarine landslides contributed to these deposits. The non-deposition of Unit B further south infers that bottom currents must have been shifted southwards and that bottom current velocities were high there. An interpolation of deposit distribution together with bathymetric data in Fig. 9 clarifies that Unit B was only deposited in shallower areas on the Chatham Rise slope. Interpolations along the slope can possibly be extended between more distant profiles as illustrated by brick-pattern areas in Fig. 9.

Profiles P7 and P8 show small Unit B deposits suggesting the presence of strong erosive currents that either limited deposition or eroded more extensive deposits to produce the remnants recorded in the profiles (e.g. Fig. 7B). After a period of drift accumulation, which was initiated after the widespread erosion of the 'Marshall Paraconformity' and continued until the early Miocene, Carter et al. (2004) suggest an interruption of drift deposition by several erosional phases that coincided with an expansion of the East Antarctic Ice Sheet, an increase of AABW production (cf. Hall et al., 2001) and/or the strengthening and northward migration of the ACC towards the eastern Chatham Rise. Due to the lower elevation of West Antarctica, most of the West Antarctic Ice Sheet expanded not earlier than the middle Miocene together with an expansion of sea-ice (e.g. Uenzelmann-Neben and Gohl, 2014), which likely caused a further increase in AABW production and bottom-current intensity through the SW Pacific.

Deposits of Unit B between the profiles P9 and P13 show wavy, subparallel internal reflectors. This points to a less dynamic depositional environment than discussed previously. Internal onlaps imply minor, small-scale changes of the current regime, for example the formation of eddies possibly shed from the over-riding ACC during cold periods (cf. Stanton and Morris, 2004). Onlaps and downlaps of Unit B to Unit C suggest a migration of the former towards Chatham Rise.
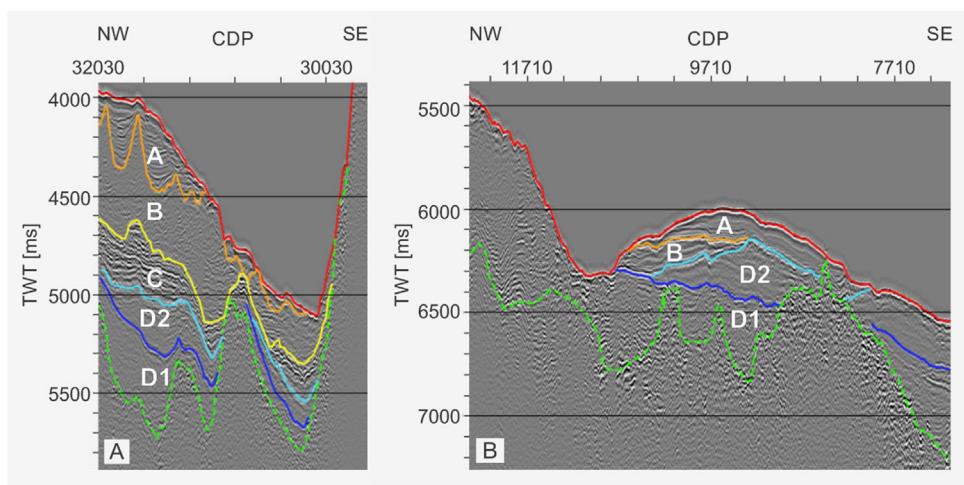
Fig. 7. A: A section of profile P3, showing the downslope area with seismic interpretation. The boundary between Unit C and Unit B is marked by a distinct unconformity (yellow line) called the 'Marshall Paraconformity'. An erosional upper surface of Unit C indicates high bottom current velocities after the opening of the Tasmanian Gateway.

B: A section of profile P7 with seismic interpretation. In this part of the profile, Unit C has been removed so that erosion extends into Unit D. Small deposits of Unit B and Unit A suggest an along-slope current path. (For interpretation of the references to color in this figure legend, the reader is referred to the web version of this article.)

Furthermore, all deposit shapes of Unit B found in the profiles P9 to P13 show an upwardly convex geometry which, together with the migration of the sediment bodies, are typical characteristics for contour current depositions (Fig. 10) (Faugères et al., 1999). Horn and Uenzelmann-Neben (2015) identified drift bodies with similar characteristics in the Bounty Trough. Overall, the seismic evidence is consistent with a northward passage of the DWBC around the eastern Chatham Rise and its intensification under southern hemisphere Coriolis deflection according to Carter and McCave (1994).

5.4. Oceanographic and sedimentary conditions from 1.7 Ma to recent

Following full development of the Solander Channel, Bounty Channel and Hikurangi Channel (Fig. 1) in the Plio-Pleistocene, drift accumulation changed from biopelagic and hemipelagic to a terrigenous-dominant sedimentation (Carter et al., 2004). Along the eastern Chatham Rise margin, most of the terrigenous material was delivered by turbidity currents passing along the Bounty Channel to feed the Bounty Fan that developed into the path of the DWBC. Accordingly, parts of that sediment input moved northwards under the boundary flow (Carter and Carter, 1996; McCave and Carter, 1997).

Seismic profiles P9 to P13 exhibit internal reflectors that are wavy, subparallel and closely spaced (Fig. 10). These are similar to Unit B, suggesting a similar depositional regime. Erosional truncations in several profiles suggest high current velocities along the eastern Chatham Rise slope and within current channels and moats formed against seamounts (Fig. 11: channels f–i). Another indicator for the existence of channels is the mounded geometry of all sediment bodies with depressions next to the slope, as described for elongate-mounded contouritic drifts by Faugères et al. (1999) and Rebesco et al. (2014)
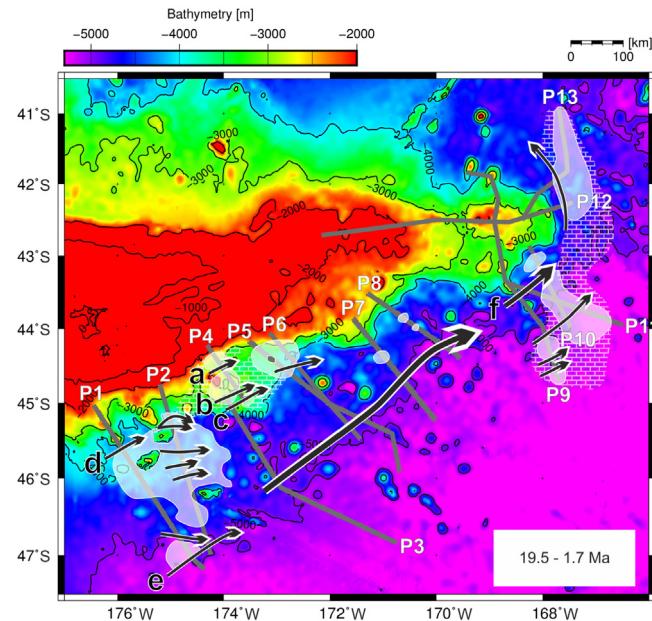
Fig. 9. Interpolated locations of sediment depositions of Unit B are illustrated by white areas. Brick-pattern areas represent interpolations between those areas. Suggested current locations are illustrated by arrows and current channels described in Sections 5.3 and 5.4 are represented by small letters. Profile lines are shown in grey.
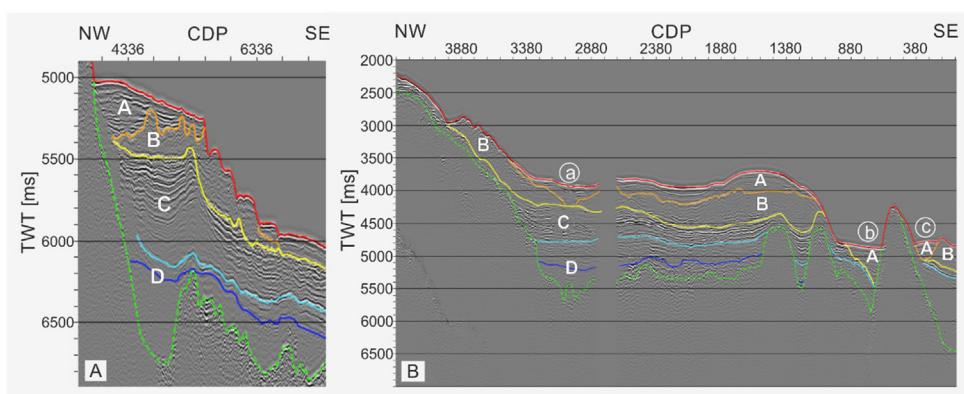
Fig. 8. A: A section of profile P5, showing the downslope area with seismic interpretation. Unit B is characterized by chaotic, wavy internal reflectors, which point to often varying current conditions. An erosional surface marks the boundary to Unit A.

B: Profile P4 with seismic interpretation. Small areas of non-deposition or erosion and channelization next to the seamount, which are marked as white circles, probably reflect localised topographic current intensification. During times of deposition of Unit A, small basin fills next to the seamount point to a cessation of channel activity.
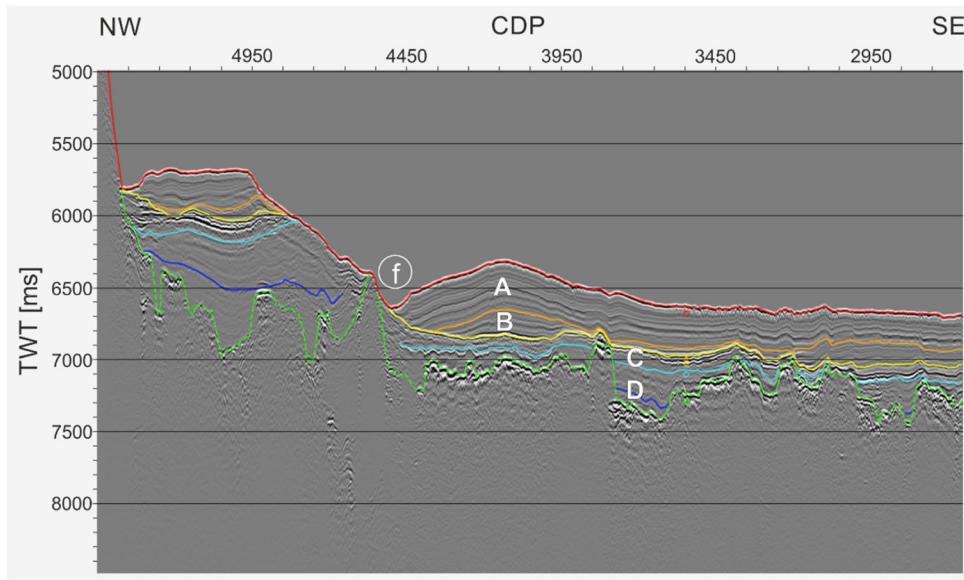
Fig. 10. A section of profile P10 with seismic interpretation. The 'Marshall Paraconformity' (yellow line) marks the boundary between Unit C and Unit B and represents the transition to a different sedimentation regime, highly influenced by along-slope bottom current activity. This is shown by erosional truncations at CDPs 5100, 4950 and 4450 (also described in chapter 5.4 and marked as white circle with small letter 'f') of Unit A and CDP 3950 of Unit B. Additionally, onlap and downlap structures in Unit A and B from CDP 4200 to 4500 suggest a drift migration due to a shifting of the current. Together with the upwardly convex geometry of the drift body these are typical characteristics for a contour current deposition (Faugères et al., 1999; Rebesco et al., 2014). (For interpretation of the references to color in this figure legend, the reader is referred to the web version of this article.)
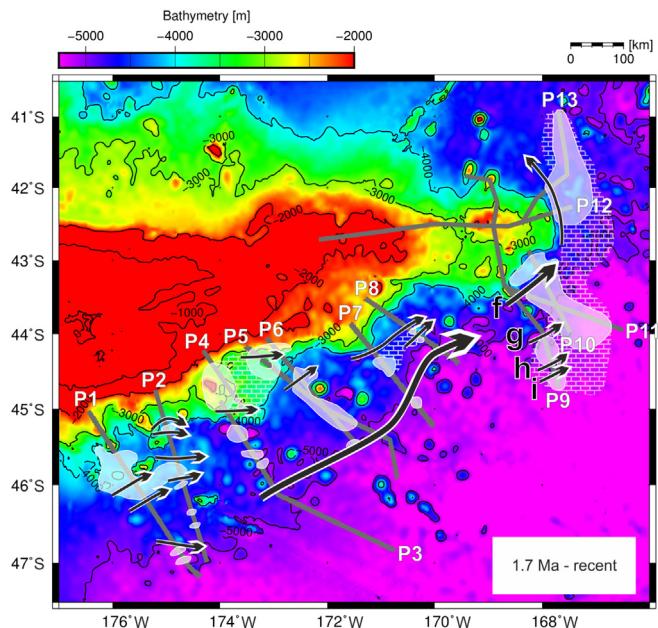
Fig. 11. Interpolated locations of sediment depositions of Unit A are illustrated by white areas. Brick-pattern areas represent interpolations between those areas. Suggested current locations are illustrated by arrows and current channels described in chapter 5.3 and 5.4 are represented by small letters. Profile lines are shown in grey.

(Fig. 10). An interpolation of Unit A between the profiles along the eastern Chatham Rise slope (Fig. 11) correlates with the description of a large sediment deposit termed the Chatham Deep Drift by Carter et al. (2004) (Fig. 1). In summary, a migration of the sediment bodies towards the Chatham Rise slope can be recognized by a downlap of internal layers in different profiles.

A very large deposit of Unit A extends between the profiles P1 and P2 (Fig. 11). In the southern section of these profiles many small Unit A deposits indicate a bottom-current influenced sedimentation regime. This is also evident by a wavy character of subparallel internal reflectors. Parasound profiles (e.g. Fig. 4) clarify that the wavy structure of internal reflectors decreased from Sub-unit A1 to Sub-unit A3, which is probably attributed to less turbulent current conditions since times of deposition of Unit B. Cessation of channel erosion is suggested from

observations of infilled small depressions on single line crossings in profiles P1 and P4, which distinctly occur next to seamounts (Figs. 8B; 9: channels b–c). Another large deposit of Unit A probably extends along the slope between P3 and P4 (cf. Fig. 7A, 8B and 11). This can be attributed to a cessation of channel transport, which has divided two deposits of Unit B in the northern part of profile P4 from each other (Figs. 8B, 9: channel a). Small depositions of Unit A in P3, as well as very large deposits of Unit A in P5 and P6 indicate either a shifting of the current path southwards or a deceleration of the current, causing a reduction in the area of more intense erosion and deposition. However, a small deposit with downlapping wavy reflectors in P5 still points to the existence of along-slope currents in shallower regions.

The profiles P7 and P8 show a less common distribution of Unit A in small mounded deposits (e.g. Fig. 7B). This might be attributed to a narrowing and therefore intensification of the bottom currents due to steepening of the slope (Fig. 11). Nevertheless, the bathymetry between both profiles suggests a continuity between sediment deposition comprising Unit A in P7 and two deposits in P8, which are locally separated by a seamount. Erosional truncations next to the slope and downlap structures next to seamounts indicate the existence of an along-slope current as previously described for this area as well as branching of the current around seamounts.

6. Conclusions

Seismic data analysis allows the reconstruction of ocean current conditions along the southeastern Chatham Rise margin for the past 80 Myr. From ~80 Ma to 33.7 Ma, post-Gondwana break-up sedimentation of the southeastern Chatham Rise margin resulted in mostly regular drape-like deposition indicating generally quiescent benthic current conditions. However, some internal discontinuities point to the occurrence of a proto-DWBC, which passed north-eastward through the study area and indicates some vigour of a SW Pacific Ocean circulation despite its relative isolation. The deep-water opening of the Tasmanian Gateway at 33.5 Ma strongly influenced the development of the Pacific DWBC and caused widespread erosion and non-deposition and the formation of the Oligocene 'Marshall Paraconformity' (Carter et al., 2004). During the Miocene, bottom current conditions in the western part of the study area often changed as indicated by chaotic wavy internal reflectors, eroded depositional units and internal onlaps attesting to intermittent erosion and deposition. In the eastern part of the study area, migration of sediment bodies towards the Chatham Rise and an upwardly convex geometry of these bodies indicate the presence of an

element of the DWBC around southeastern Chatham Rise from Miocene to recent times. Intensification of the DWBC in the Miocene onwards is consistent with an increase in Antarctic glaciation and formation of AABW together with periodic strengthening of the ACC. Development of three major sediment channel systems extending from New Zealand in the Plio-Pleistocene led to a terrigenous-dominant sedimentation, especially during glacial periods (e.g. Carter et al., 2004). Although large gaps remain between the widely-spaced seismic reflection profiles, this study enables a detailed time-dependent mapping and reconstruction of ocean-bottom current related sediment deposits along the southeastern Chatham Rise revealing new insights into the dynamics of the SW Pacific circulation.

Declaration of competing interest

The authors declare that they have no known competing financial interests or personal relationships that could have appeared to influence the work reported in this paper.

Acknowledgements

References

Carter, R.M., Carter, L., 1996. The abyssal bounty fan and lower Bounty Channel: evolution of a rifted-margin sedimentary system. Mar. Geol. 130, 181–202. https://doi.org/10.1016/0025-3227(95)00139-5.

Carter, R.M., Landis, C.A., 1972. Correlative oligocene unconformities in southern Australasia. Nat. Phys. Sci. 237, 12–13. https://doi.org/10.1038/physci237012a0.

Carter, L., McCave, I.N., 1994. Development of sediment drifts approaching an active plate margin under the SW Pacific Deep Western Boundary Current. Paleoceanography 9, 1061–1085. https://doi.org/10.1029/94PA01444.

Carter, L., McCave, I.N., 2002. Eastern New Zealand Drifts, Miocene-Recent. Geol. Soc. Lond. Mem. 22, 385–407. https://doi.org/10.1144/GSL.MEM.2002.022.01.27.

Carter, L., Wilkin, J., 1999. Abyssal circulation around New Zealand – a comparison between observations and a global circulation model. Mar. Geol. 159, 221–239. https://doi.org/10.1016/S0025-3227(98)00205-9.

Carter, R.M., Carter, L., Davy, B., 1994. Seismic stratigraphy of the Bounty Trough, southwest Pacific Ocean. Mar. Pet. Geol. 11, 79–93. https://doi.org/10.1016/0264-8172(94)90011-6.

Carter, R.M., Carter, L., McCave, I.N., 1996. Current controlled sediment deposition from the shelf to the deep ocean: the Cenozoic evolution of circulation through the SW Pacific gateway. Geol. Rundsch. 85, 438–451. https://doi.org/10.1007/BF02369001.

Carter, R.M., McCave, I.N., Richter, C., Carter, L., Aita, Y., Buret, C., Di Stefano, A., Fenner, J., Fothergill, P., Gradstein, F., Hall, I., Handwerger, D.A., Harris, S., Hayward, B., Hu, S., Joseph, L., Khim, B.K., Millwood, L., Rinna, J., Smith, G., Suzuki, A., Weedon, G., Wei, K., Wilson, G., Winkler, A., 1999. Site 1122: turbidites with a contourite foundation. In: Carter, R. M., McCave, I. N., Richter, C., Carter, L., et al., Proc ODP, Initial Reports, 181. Ocean Drilling Program, College Station, TX, pp. 1–146.

Carter, L., Carter, R.M., McCave, I.N., 2004. Evolution of the sedimentary system beneath the deep Pacific inflow off eastern New Zealand. Mar. Geol. 205, 9–27. https://doi.

org/10.1016/S0025-3227(04)00016-7.

Eagles, G., Gohl, K., Larter, R.D., 2004. High-resolution animated tectonic reconstruction of the South Pacific and West Antarctic margin. Geochem. Geophys. Geosystems 5. https://doi.org/10.1029/2003GC000657.

Exon, N.F., Kennett, J.P., Malone, M.J., 2004. The Cenozoic Southern Ocean: tectonics, sedimentation, and climate change between Australia and Antarctica. Geophys. Monogr. Ser. 151, 367. https://doi.org/10.1029/GM151.

Faugères, J.-C., Stow, D.A.V., Imbert, P., Viana, A., 1999. Seismic features diagnostic of contourite drifts. Mar. Geol. 162, 1–38. https://doi.org/10.1016/S0025-3227(99)00068-7.

Gohl, K., Werner, R., 2016. The Expedition SO246 of the Research Vessel SONNE to the Chatham Rise in 2016, Reports on Polar and Marine Research. 698https://doi.org/10.2312/BzPM_0698_2016. 158 p.

Hall, I.R., McCave, I.N., Shackleton, N.J., Weedon, G.P., Harris, S.E., 2001. Intensified deep Pacific inflow and ventilation in Pleistocene glacial times. Nature 412, 809–812. https://doi.org/10.1038/35090552.

Horn, M., Uenzelmann-Neben, G., 2015. The Deep Western Boundary Current at the Bounty Trough, east of New Zealand: indications for its activity already before the opening of the Tasmanian Gateway. Mar. Geol. 362, 60–75. https://doi.org/10.1016/j.margeo.2015.01.011.

Kennett, J.P., Burns, R.E., Andrews, J.E., Churkin, M., Davies, T.A., Dumitrica, P., Edwards, A.R., Galehouse, J.S., Packham, G.H., van der Lingen, G.J., 1972. Australian-Antarctic continental drift, paleocirculation changes and Oligocene deepsea erosion. Nature Phys. Sci. 239, 51–55.

Larter, R.D., Cunningham, A.P., Barker, P.F., Gohl, K., Nitsche, F.O. (2002). Tectonic evolution of the Pacific margin of Antarctica - 1. Late Creataceous tectonic reconstructions. J. Geoph. Res. *107*, B12, doi: https://doi.org/10.1029/2000JB000052.

McCave, I.N., Carter, L., 1997. Recent sedimentation beneath the Deep Western Boundary Current of northern New Zealand. Deep Sea Res. Part Oceanogr. Res. Pap. 44, 1203–1237. https://doi.org/10.1016/S0967-0637(97)00011-3.

Mortimer, N., van den Bogaard, P., Hoernle, K., Timm, C., Gans, P.B., Werner, R., Riefstahl, F., 2019. Late Cretaceous oceanic plate reorganization and the breakup of Zealandia and Gondwana. Gondwana Res. 65, 31–42. https://doi.org/10.1016/j.gr.2018.07.010.

Orsi, A.H., Johnson, G.C., Bullister, J.L., 1999. Circulation, mixing and production of Antarctic Bottom Water. Prog. Oceanogr. 43, 55–109. https://doi.org/10.1016/S0079-6611(99)00004-X.

Rebesco, M., Hernández-Molina, F.J., Van Rooij, D., Wåhlin, A. (2014). Contourites and associated sediments controlled by deep-water circulation processes: State-of-the-art and future considerations. Mar. Geol., 50th Anniversary Special Issue *352*, 111–154, doi: 10.1016/j.margeo.2014.03.011.

Riefstahl, F., Gohl, K., Davy, B., Hoernle, K., Mortimer, N., Timm, C., Werner, R., Hochmuth, K., 2020. Cretaceous intracontinental rifting at the southern Chatham Rise margin and initialisation of seafloor spreading between Zealandia and Antarctica. Tectonophysics 776, 228298. https://doi.org/10.1016/j.tecto.2019.228298.

Sijp, W.P., England, M.H., Huber, M., 2011. Effect of the deepening of the Tasman Gateway on the global ocean. Paleoceanography 26, 1–18. https://doi.org/10.1029/2011PA002143.

Stanton, B.R., Morris, M.Y. (2004). Direct velocity measurements in the Subantarctic Front and over Campbell Plateau, southeast of New Zealand. J. Geoph. Res. *109*, C01028, doi: 1029/2002JC001339.

Stickley, C.E., Brinkhuis, H., Schellenberg, S.A., Sluijs, A., Röhl, U., Fuller, M., Grauert, M., Huber, M., Warnaar, J., Williams, G.L., 2004. Timing and nature of the deepening of the Tasmanian Gateway. Paleoceanography 19. https://doi.org/10.1029/2004PA001022.

Uenzelmann-Neben, G., Gohl, K., 2014. Early glaciation already during the Early Miocene in the Amundsen Sea, Southern Pacific: Indications from the distribution of sedimentary sequences. Glob. Planet. Chang. 120, 92–104. https://doi.org/10.1016/j.gloplacha.2014.06.004.

Uenzelmann-Neben, G., Grobys, J., Gohl, K., Barker, D., 2009. Neogene sediment structures in Bounty Trough, eastern New Zealand: Influence of magmatic and oceanic current activity. GSA Bull. 121, 134–149. https://doi.org/10.1130/B26259.1.

Wessel, P., Smith, W.H.F., 1998. New, improved version of generic mapping tools released. Eos, Transactions, American Geophysical Union 79, 579. https://doi.org/10.1029/98EO00426.

Whittaker, J.M., Müller, R.D., Leitchenkov, G., Stagg, H., Sdrolias, M., Gaina, C., Goncharov, A., 2007. Major Australian-Antarctic plate reorganization at Hawaiian-Emperor bend time. Science 318, 83–86. https://doi.org/10.1126/science.1143769.

Whittaker, J.M., Williams, S.E., Müller, R.D., 2013. Revised tectonic evolution of the Eastern Indian Ocean. Geochem. Geophys. Geosystems 14, 1891–1909. https://doi.org/10.1002/ggge.20120.

Whitworth, T., Warren, B.A., Nowlin, W.D., Rutz, S.B., Pillsbury, R.D., Moore, M.I., 1999. On the deep western-boundary current in the Southwest Pacific Basin. Prog. Oceanogr. 43, 1–54. https://doi.org/10.1016/S0079-6611(99)00005-1.

Wobbe, F., Gohl, K., Chambord, A., Sutherland, R., 2012. Structure and breakup history of the rifted margin of West Antarctica in relation to Cretaceous separation from Zealandia and Bellingshausen plate motion. Geochem. Geophys. Geosystems 13, 1–19. https://doi.org/10.1029/2011GC003742.